Mon. Not. R. Astron. Soc. **000**, 000–000 (0000) Printed 15 April 2009 (MN LATEX style file v1.4)

Dual black holes in merger remnants. I: linking accretion to dynamics.

M. Dotti[1,2⋆], M. Ruszkowski[1,3], L. Paredi[2], M. Colpi[4], M. Volonteri[1], F. Haardt[2]

[1] *Department of Astronomy, University of Michigan, Ann Arbor, MI, 48109, USA*
[2] *Dipartimento di Fisica e Matematica, Università dell'Insubria, Via Valleggio 11, 22100 Como, Italy*
[3] *The Michigan Center for Theoretical Physics, Ann Arbor, MI, 48109, USA*
[4] *Dipartimento di Fisica G. Occhialini, Università degli Studi di Milano Bicocca, Piazza della Scienza 3, 20126 Milano, Italy*

15 April 2009

ABSTRACT

We study the orbital evolution and accretion history of massive black hole (MBH) pairs in rotationally supported circumnuclear discs up to the point where MBHs form binary systems. Our simulations have high resolution in mass and space which, for the first time, makes it feasible to follow the orbital decay of a MBH either counter– or co–rotating with respect to the circumnuclear disc. We show that a moving MBH on an initially counter–rotating orbit experiences an "orbital angular momentum flip" due to the gas-dynamical friction, i.e., it starts to corotate with the disc before a MBH binary forms. We stress that this effect can only be captured in very high resolution simulations. Given the extremely large number of gas particles used, the dynamical range is sufficiently large to resolve the Bondi-Hoyle-Lyttleton radii of individual MBHs. As a consequence, we are able to link the accretion processes to the orbital evolution of the MBH pairs. We predict that the accretion rate is significantly suppressed and extremely variable when the MBH is moving on a retrograde orbit. It is only after the orbital angular momentum flip has taken place that the secondary rapidly "lights up" at which point both MBHs can accrete near the Eddington rate for a few Myr. The separation of the double nucleus is expected to be around $\lesssim 10$ pc at this stage. We show that the accretion rate can be highly variable also when the MBH is co–rotating with the disc (albeit to a lesser extent) provided that its orbit is eccentric. Our results have significant consequences for the expected number of observable double AGNs at separations of $\lesssim 100$ pc.

Key words: black hole physics – hydrodynamics – galaxies: starburst – galaxies: evolution – galaxies: nuclei

1 INTRODUCTION

In recent years, compelling observational evidence has indicated that massive black holes (MBHs) are ubiquitous in nuclei of local bright galaxies (Richstone et al. 1998; Marconi et al. 2004; Shankar et al. 2004; Ferrarese et al. 2006; Ferrarese 2006; Decarli et al. 2007). According to the structure formation paradigm, galaxies often interact and merge as their dark matter halos assemble in a hierarchical fashion, and the MBHs, incorporated through mergers, are expected to grow, evolve and *pair* with other MBHs (Begelman Blandford & Rees 1980; Volonteri, Haardt, & Madau 2003). The formation of MBH pairs thus appears to be an inevitable and natural consequence of galaxy assembly.

A large number of merging systems such as the luminous infrared galaxies (LIRGs) hosts a central rotationally supported massive (up to 10^{10}M$_\odot$) gaseous disc extending on scales of ~ 100 pc (Sanders & Mirabel 1996; Downes & Solomon 1998; Davies et al. 2004). These discs may be the end–product of gas–dynamical, gravitational torques excited during the merger, when a large amount of gas is driven into the core of the remnant (Mayer et al. 2007). Inside a massive self–gravitating disc, a putative MBH pair can continue its dynamical evolution and, possibly, accrete gas producing a double AGN (Kocsis et al. 2005, Dotti et al. 2006a).

The possibility of double accretion processes during the different stages of a galaxy merger is still a matter of debate.

⋆ e-mail address: mdotti@umich.edu

From an observational point of view, only few tens of double quasars are known (with separations $\lesssim 100$ kpc; see e.g. Foreman, Volonteri & Dotti 2008 and references therein). There are only a few well studied cases of ongoing mergers at sub-galactic scales in which each companion is an AGN. Examples of such systems include NGC 6240 (Komossa et al. 2003), Arp 229 (Ballo et al. 2004), and Mrk 463 (Bianchi et al. 2008). Other two dual AGN candidates with separation ~ 1 kpc have been identified spectroscopically by Comerford et al. (2008). On parsec scale, only one resolved active MBH binary has been found in the nucleus of the elliptical galaxy 0402+369 (Rodriguez et al. 2006), and the existence of two more sub–parsec MBH binary candidates has been suggested (OJ287, Valtonen et al. 2007, and SDSSJ092712.65+294344.0, Bogdanovic, Eracleous & Sigurdsson 2008; Dotti et al. 2008).

Accretion events during the last phases of a MBH binary (for sub–parsec separations) have been studied in detail by several authors (Armitage & Natarajan 2002, 2005; Hayasaki, Mineshige, & Sudou 2007; Hayasaki, Mineshige, & Ho 2008; Cuadra et al. 2009). On larger scales, the possibility of gas accretion during the MBH pairing has been recently studied using numerical simulations in the context of galaxy mergers (e.g., Kazantzidis et al. 2005; Springel et al. 2005; Di Matteo et al. 2005; Hopkins et al. 2005; Hopkins et al. 2006). In these works, the authors study a galaxy-galaxy collision on spatial scales of ~ 100 kpc, and the number of particles used to model the two galaxies does not allow them to resolve the influence radii of the two pairing MBHs. This lack of resolution prevents the authors from accurately predicting the accretion rates onto the two MBHs. Given the limits of the currently available supercomputers, such simulations would be prohibitively time consuming. Therefore, no simulations resolving the Bondi-Hoyle-Lyttleton radii during a complete galaxy–galaxy merger have been published to date.

We have run a suite of high resolution N–body/hydrodynamical simulations of MBH pairing in circumnuclear discs. In this paper we discuss the dynamical evolution of the MBH pairs up to a point where they form a binary (i.e., up to a point where the mass enclosed inside the MBH orbit is smaller than the sum of the MBH masses). We follow the MBH dynamics from an initial separation of 50 pc down to sub–parsec separation while resolving $R_{\rm BHL}$ of the two pairing MBHs. We predict the accretion rate onto the two MBHs as a function of the geometry of the merger. As we demonstrate in this paper, this approach allows us to study the possibility that a galaxy merger event may be associated with a single or double active galactic nucleus depending on the configuration of the initial MBH orbits. It also allows us to constrain the fate of the MBH binary (i.e., coalescence vs. stalling). The evolution of the MBH spins and the fate of the newly formed MBH binary will be discussed in two forthcoming papers.

2 SIMULATION SETUP

We follow the dynamics of MBH pairs in nuclear discs using numerical simulations run with the N–Body/SPH code GADGET (Springel, Yoshida & White 2001), upgraded to include the accretion physics. The main input parameters of our simulations are summarized in Table 1.

Table 1. Run parameters

run	prograde ?	e_i	γ
HPC	yes	0	
HPE	yes	0.7	5/3, "hot"
HRE	no	0.7	
CPC	yes	0	
CPE	yes	0.7	7/5, "cold"
CRE	no	0.7	

The initial conditions of our runs are set following the procedure discussed in Dotti, Colpi & Haardt (2006b) and Dotti et al. (2007). In our models, two MBHs are placed in the plane of a gaseous disc, embedded in a larger stellar spheroid. The gaseous disc is modeled with 2,353,310 particles, has a total mass $M_{\rm Disc} = 10^8 {\rm M}_\odot$, and follows a Mestel surface density profile

$$\Sigma(R) = \frac{M_{\rm disc}}{2\pi R_{\rm disc} R} \tag{1}$$

where R is the radial distance projected into the disc plane and $R_{\rm disc} = 100$ pc is the size of the disc. The disc is rotationally supported in R and has a vertical thickness of 10 pc. Initially, the gaseous particles are distributed uniformly along the vertical axis. The internal energy per unit mass of the SPH particles scales as:

$$u(R) = K R^{-2/3}, \tag{2}$$

where K is a constant defined so that the Toomre parameter of the disc,

$$Q = \frac{\kappa c_{\rm s}}{\pi G \Sigma}, \tag{3}$$

is ≥ 3 everywhere, preventing the fragmentation of the disc (the average value of Q over the disc surface is ≈ 10). In equation (3) κ is the local epicyclic frequency, and $c_{\rm s}$ is the local sound speed of the gas. Gas is evolved adiabatically assuming a polytropic index $\gamma = 5/3$ or $\gamma = 7/5$. In the former case, the runs are denoted by "1" and are termed "hot" as the temperature is proportional to a higher power of density than in the latter class of runs ("cold" cases, runs denoted by "2"). The hot case corresponds to adiabatic monoatomic gas, while the cold has been shown to provide a good approximation to a solar metallicity gas heated by a starburst (Spaans & Silk 2000; Klessen, Spaans, & Jappsen 2007).

The spheroidal component (bulge) is modeled with 10^5 collisionless particles, initially distributed as a Plummer sphere with mass density profile

$$\rho(r) = \frac{3}{4\pi} \frac{M_{\rm Bulge}}{b^3} \left(1 + \frac{r^2}{b^2}\right)^{-5/2}, \tag{4}$$

where b (= 50 pc) is the core radius, r the radial coordinate, and $M_{\rm Bulge} (= 6.98 M_{\rm Disc})$ is the total mass of the spheroid. With such a choice, the mass of the bulge within 100 pc is five times the mass of the disc, as suggested by Downes & Solomon (1998).

The two MBHs (M_1 and M_2) are equal in mass ($M_{\rm BH} =$

4×10^6 M$_\odot$). The initial separation of the MBHs is 50 pc. M_1, called primary for reference, is placed at rest at the centre of the circumnuclear disc. The secondary (denoted as M_2) is either corotating with the gaseous disc on a circular orbit, or moving on an eccentric counterrotating or corotating orbit with respect to the circumnuclear disc. For eccentric orbits, the initial ratio between the absolute values of the radial and tangential velocity of M_2 is $v_{\rm rad}/v_{\rm tan} = 3$. This ratio sets the eccentricity of the first orbit of M_2 to $e \simeq 0.7$. Given the large masses of the disc and the bulge, the dynamics of the moving MBH (M_2) is uneffected by the presence of M_1 until the MBHs form a gravitationally bound system. The subsequent evolution of the MBH binary will be discussed in a forthcoming paper.

We evolve our initial composite model (bulge, disc and M_1) for ≈ 3 Myrs, until the bulge and the disc reach equilibrium, as described in Dotti et al. (2006b; 2007). The disc, having initially finite thickness and homogeneous vertical density distribution, is allowed to relax to an equilibrium configuration along the z–axis. The new distribution of the gas in the disc in the z direction becomes non-uniform once the equilibrium configuration is reached. The new disc has a vertical thickness of ≈ 8 pc (defined as containing 90% of the mass in the vertical direction at every radius) This thickness is independent of the radius and is $\approx 4/5$ of the initial un–relaxed value.

We allow the gas particles to be accreted onto the MBHs if the following two criteria are fulfilled:

- the sum of the kinetic and internal energy of the gas particle is lower than α times the absolute value of its gravitational energy (all the energies are computed with respect to each MBH)
- the total mass accreted per unit time onto a MBH every timestep is lower than the accretion rate corresponding to the Eddington luminosity ($L_{\rm Edd}$) computed assuming a radiative efficiency (ϵ) of 10%.

The parameter α is a constant defining how much a particle has to be bound to a MBH to be accreted. We set $\alpha = 0.3$. Note that due to the nature of the above criteria, the gas particles can accrete onto the MBHs only if the Bondi-Hoyle-Lyttleton radius, defined as

$$R_{\rm BHL} = \frac{G\,M}{v_{\rm rel}^2 + c_{\rm s}^2}, \qquad (5)$$

is resolved in the simulations. In Eq. (5), M is the mass of the MBH, $v_{\rm rel}$ is the relative velocity between the gas and the moving MBH, and $c_{\rm s}$ is the sound speed of the gas. M is evolved by adding at each timestep $1-\epsilon$ times the total mass of the accreted gas particles. If the amount of bound gas particles implies super–Eddington accretion, the code randomly selects a subsample of the particles within $R_{\rm BHL}$ to be accreted, so as to prevent accretion from reaching super-Eddington rates. This simplified treatment of the black hole feedback does not capture effects such as the accretion driven wind, and its effect on the environment. Because the MBHs accrete only a small fraction of their initial masses ($< 10\%$) during our simulations, AGN feedback is not expected to modify the global properties of the circumnuclear disc. Nevertheless, such feedback can remove a fraction of the gas a few parsecs away from MBHs accreting near the Eddington limit. This could decrease the accretion rate onto the MBHs and the efficiency of MBH pairing after they form a binary system. The accurate implementation of a self–consistent radiative feedback is beyond the scope of this work, and will be the subject of our future studies.

The number of neighboring SPH particles adopted in our simulation is $N_{\rm neigh} = 32$. The resulting spatial resolution of the hydrodynamical force in the highest density regions is ≈ 0.1 pc. In order to prevent numerical errors due to the density-dependent effective resolution, we set both the gravitational softening of the gaseous particles and that of the MBHs to 0.1 pc. With this spatial resolution we can resolve the vertical scale of the disc and, as a consequence, we can calculate angular momentum transport due to disc self–gravity (see, e.g., Lodato & Rice 2004; Nelson 2006). We can also resolve the influence radius of M_1 (≈ 1 pc) and M_2, a condition necessary to study the gas accretion onto MBHs [†].

In addition, our accretion scheme is such that linear momentum is conserved. This includes automatically the braking exerted by the accretion flow onto the moving MBH ($\mathbf{F}_{\rm BHL} = \dot{M}\,\mathbf{v}_{\rm rel}$, where $\dot{M}$ is the accretion rate). The only viscosity term in the simulations is the shear reduced version (Balsara 1995; Steinmetz 1996) of the standard Monaghan and Gingold (1983) artificial viscosity.

3 RESULTS

3.1 Orbital evolution

In this Section we discuss the orbital evolution of the pairs in six different runs, until the MBHs form a binary. The relationship between the orbital properties of the MBHs and their accretion properties is discussed in Section 3.2. The run names and parameters are listed in Table 1. The letters used to name the runs encode the type of the run with the first, second and third letter corresponding to hot vs. cold, prograde vs. retrograde and eccentric vs. circular cases, respectively. For example, CRE corresponds to a secondary MBH on an eccentric retrograde orbit in a cold disk.

3.1.1 Prograde orbits

The pairing process of MBHs on circular orbits (runs HPC and CPC) brings the two MBHs down to separations $\lesssim 5$ pc in less than 10 Myrs at which point they form a binary. The MBHs orbital decay proceeds without any observable eccentricity growth. Because of the low relative velocity between the MBH and the gas, M_2 interacts efficiently with the gas out to a distance of a few parsecs. In this case, the dynamical evolution of the pair is almost indistinguishable from lower (parsec scale) resolution simulations (Escala et al. 2005; Dotti et al. 2006b; Dotti et al. 2007), before the MBHs bind in a binary.

The upper panel of Fig. 1 shows the separation between the two MBHs as a function of time for M_2 moving initially on a prograde eccentric orbit inside the hot disc ($\gamma = 5/3$,

[†] Note that $R_{\rm BHL}$ of M_2 depends on the phase of its orbit. That is, $R_{\rm BHL}$ depends on the relative MBH–gas velocity, which is different in the corotating and counterrotating cases.

run HPE). The two MBHs reach a separation of the order of $\lesssim 10$ pc in less than 5 Myr. The MBH pair loses memory of its initial eccentricity in the early phases of the orbital decay. Such circularization is due to the variation in direction and in magnitude of dynamical friction acting on M_2 during an orbital period. Dynamical friction tends to slow down the secondary near the periastron and to accelerate it at the apoastron (see Dotti et al. 2006b; Dotti et al. 2007 for a detailed discussion). The orbital decay and circularization observed in these high resolution runs are slightly faster than in the low resolution simulations presented in Dotti et al. (2006b) and Dotti et al. (2007). The increased resolution allows to better resolve the interaction between the gas environment and M_2 when it is still moving on eccentric orbits and the relative velocity between M_2 and the gas particles is high. This effect of the increased resolution is more prominent for retrograde orbits, where the relative velocities are higher. We postpone a detailed discussion of this effect to Section 3.1.2.

The thermodynamics of the gas also has impact on the circularization process. The dynamical interaction of the moving MBH of mass M_2 with the gas is stronger in a cold disc. This is especially so when the secondary is corotating with the disc. The reason for this is that the relative velocity between the secondary and the disc material is small in this case (at least for circular orbits) and the Bondi-Hoyle-Lyttleton radius reduces to the Bondi radius which is proportional to c_s^{-3}, where c_s is the sound speed. It is for this reason that the orbital decay and the circularization in a cold disc (run CPE) proceeds faster than in the hot case. In our simulations dynamical friction is efficient in reducing the eccentricity down to values < 0.1, for both cold and hot cases.

3.1.2 Retrograde orbits

For the retrograde cases (runs HRE and CRE) we find that the two MBHs also reach a separation of $\lesssim 10$ pc in less than 5 Myr, as illustrated in the upper panels of Fig. 2 and Fig. 3. The middle panels of Fig. 2 and Fig. 3 show the evolution of the z–component of the orbital angular momentum L_z of M_2 normalized to its initial value. The (initially negative) angular momentum grows very fast during the first Myr. As long as M_2 is counter–rotating, the MBH–disc interaction brakes the secondary even at the apocentre, because the MBH velocity and disc flow are anti–aligned there. The increase of the orbital angular momentum of M_2 is further facilitated by the fact that, while the orbit decays, the MBH interacts with progressively denser regions of the disc closer to the primary. Eventually, at about 2 Myr, the sign of the orbital momentum of the secondary changes. The dynamical friction process is the ultimate cause of this orbital angular momentum flip. After the orbital angular momentum flip has taken place and the secondary enters a co–rotating orbit with respect to the disc, the angular momentum continues to grow up to $L/L_0 \approx 0.1$.

The orbital decay of a retrograde MBH (runs HRE and CRE), and the orbital angular momentum flip process are dependent on the numerical resolution. We stress that the orbital angular momentum flip is not seen in lower resolution simulations. This resolution dependence

has a simple dynamical explanation. The perturbation

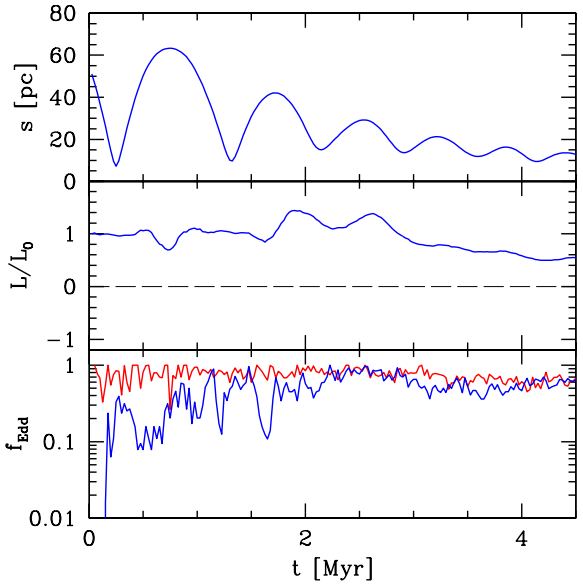

Figure 1. Run HPE. Upper panel: MBH separation as a function of time. Middle panel: time evolution of the orbital angular momentum of M_2 (L) normalized to its initial value (L_0). The thin–dashed horizontal line marks $L = 0$. Lower panel: Eddington accretion ratio as a function of time. Red and blue lines refer to M_1 and M_2, respectively.

of the orbit of a single gas particle that is caused by M_2 depends on the relative velocity between the gas and the MBH and their relative separation. Only those gas particles that get perturbed can contribute to the orbital decay of the MBH and lead to its orbital angular momentum flip. A natural scale lenght for the gravitational interaction between the MBH and gas particles is $R_{\rm BHL}$.

Gas particles can efficiently exchange angular momentum with the hole only if they pass closer to the MBH than a few $R_{\rm BHL}$.

As long as the MBH is counter–rotating, its relative velocity with respect to the disc is $v_{\rm rel} \gtrsim 200$ km s$^{-1} \gg c_s$, which corresponds to $R_{\rm BHL} \lesssim 1$ pc. Therefore, higher numerical resolution is required to model counter–rotating cases than the co–rotating ones. Given the high resolution of our simulations, the gravitational interaction is accurately computed down to scales of ≈ 0.1 pc, allowing us to correctly model the dynamical evolution of counter–rotating MBHs.

3.2 Accretion history

In run HPC the Eddington ratio $f_{\rm Edd} \equiv \dot{M}/\dot{M}_{\rm Edd}$ of the primary is ≈ 1 at the beginning of the simulation and decreases monotonically during the pairing process down to ≈ 0.7 at 5 Myr. The Eddington ratio of the primary decreases steadily because the orbital motion of the secondary heats up the gas in the vicinity of the primary. The increase in the gas temperature decreases the Bondi radius of the primary and evacuates gas from the central regions of the disc. Both of these effects reduce the accretion rate onto the primary. This effect is present only when the polytropic index $\gamma = 5/3$, as

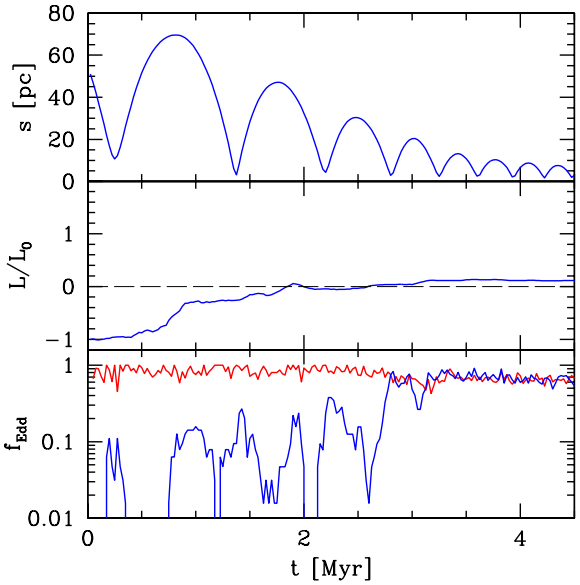

Figure 2. Same as Fig. 1 for run HRE. In the middle panel the initial angular momentum is considered negative since M_2 is initially orbiting on a retrograde orbit.

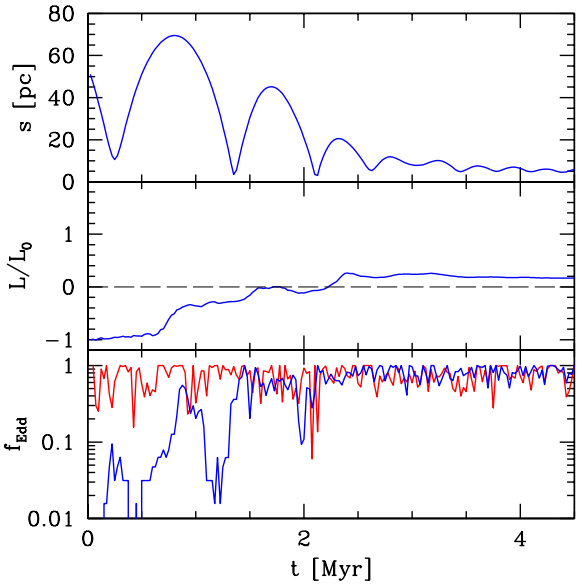

Figure 3. Same as Fig. 1 and Fig. 2 for run CRE.

in that case the increase of the gas temperature with density is larger than in the cold case where $\gamma = 7/5$ (run CPC). In the cold run, the lower value of γ allows for the pairing of the MBHs while preventing a strong heating of the gas. In both runs (HPC and CPC), M_2 has an accretion history similar to M_1. That is, MBHs on circular corotating orbits have low relative velocities with respect to the gas which leads to high and steady accretion rates.

Figures 1, 2 and 3 allow to compare directly the dynamical properties of the two MBHs to the accretion rates in runs HPE, HRE, and CRE, respectively. Top panels show the evolution of the MBH separation. Middle panels present the time dependence of the orbital angular momentum of M_2. The bottom panels show $f_{\rm Edd}$ for the primary (red lines) and secondary (blue lines) MBHs.

In runs HPE and HRE, the primary accretes at an average $f_{\rm Edd} \approx 0.7$, slightly decreasing with time. The accretion rate of the secondary evolves differently. Its accretion behaviour depends on whether it is on a co–rotating or counter–rotating orbit. In the co–rotating case (run HPE), the average $f_{\rm Edd}$ of the secondary is ≈ 0.4 during the first 5 Myr and its accretion history can be divided into two phases:

i) for $t \lesssim 2.5$ Myr the circularization process is efficient while $f_{\rm Edd} \approx 0.3$ on average and shows strong variability

ii) for $t \gtrsim 2.5$ Myr, M_2 moves on a quasi–circular orbit, and the relative velocity between M_2 and the gaseous disc is reduced. In this phase, $f_{\rm Edd} \approx 0.45$.

In the counter–rotating case (run HRE), we can still distinguish two phases albeit with some important differences:

i) for $t \lesssim 3$ Myr, M_2 is counter–rotating ($L_{\rm z} < 0$), and $f_{\rm Edd} \sim 0.05 \div 0.1$. This level of accretion is lower than in the corresponding first orbital stage in the co–rotating case described above. Moreover, the variability in the accretion rate onto the secondary MBH is now significantly larger.

ii) At $t \sim 3$ Myr the orbital angular momentum flip takes place. Thereafter, M_2 accretes at $f_{\rm Edd} \sim 0.7$. In this second stage, the main difference between the co–rotating and the counter–rotating cases is that, in the latter, M_2 exhibits a rapid transition/increase in the accretion rate (cf. bottom panels in Fig. 2 (counter–rotating case) and Fig 1 (co-rotating case). In the next subsection we present the Fourier analysis of the accretion history of M_2, in order to assess whether the variability of $f_{\rm Edd}$ is physical or it depends on numerical fluctuations due to finite number of particles used.

In run CRE, M_2 has a similar accretion history to the one observed in run HRE, but the timescale for the orbital angular momentum flip is shorter. Lower γ corresponds to colder and denser gas and, thus, more efficient dynamical friction. This makes M_2 corotate in less than 2 Myr. The primary has an average $f_{\rm Edd} \approx 0.9$, which is higher than in runs HPE and HRE. The physical reason for the enhancement in the accretion rate in the cold case is provided in the discussion.

3.2.1 Fourier analysis of accretion fluctuations in run HRE

As discussed above, strong fluctuations of $f_{\rm Edd}$ are a distinctive feature of counter–rotating (and eccentric co–rotating) MBHs. The variability is higher for counter–rotating MBHs and $f_{\rm Edd} < 0.1$ (see Fig. 2 and 3). These values of $f_{\rm Edd}$ correspond to less than a few hundred SPH particles accreted every 2.5×10^4 yr which is the time resolution in Fig. 2 and 3. Such a small number of particles is $\lesssim 10 \times N_{\rm neigh}$, and can drop down to 0 when the $R_{\rm BHL}$ of M_2 is not resolved. As a consequence, values of $f_{\rm Edd} < 0.1$ should be considered order of magnitude estimates.

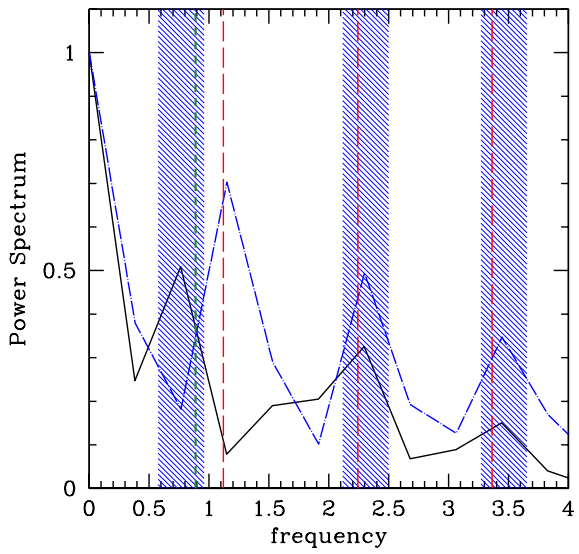

Figure 4. Power spectrum P of $f_{\rm Edd}$ fluctuations of M_2 in run HRE, until the MBH is counter–rotating with respect to the circumnuclear disc. Solid black line: P of the original $f_{\rm Edd}$. Dot–dashed blue line: P of the larger scale/noise free estimate of the $f_{\rm Edd}$ discussed in the text. P has been normalized to its value at $\nu = 0$, ν is in units of the average between $\nu_1 = 1/\tau_1$ and $\nu_2 = 1/\tau_2$. Short dashed green line marks $\nu = \nu_1$, long dashed red lines shows $\nu = \nu_2$ and its higher harmonics. The dashed regions show the values of ν compatible with the peaks of P (i.e. the frequencies of the peaks $\pm\, 1/2\,\nu_{\rm min}$).

In order to check whether the variability of $f_{\rm Edd}$ is due to finite sampling of the medium or if it has a physical meaning, we performed the Fourier analysis for run HRE[‡]. We emphasise that run HRE is the run with the lowest $f_{\rm Edd}$, i.e., most affected by the numerical errors. Therefore our conclusions will be conservative and robust.

The black solid line in Fig. 4 refers to the power spectrum (P) of the fluctuations of $f_{\rm Edd}$ of M_2, for run HRE. The frequency (ν) unit is defined as the average between $\nu_1 = 1/\tau_1$ and $\nu_2 = 1/\tau_2$, where τ_1 and τ_2 are the periods of the first and second orbit of M_2. P has been normalized to $P(\nu = 0)$. The frequency resolution of our results is $\nu_{\rm min} = 1/\Delta t$, where $\Delta t \approx 3$ Myr corresponds to the amount of time during which M_2 orbit is retrograde. [§]

Fig. 4 proves that P is not compatible with white noise as expected for fluctuations due only to numerical sampling. Moreover, we can distinguish four peaks in our distribution. The first peak at $\nu = 0$ is a simple consequence of the physical condition $f_{\rm Edd} \geq 0$. The remaining three peaks contain more physically useful information. Given our frequency resolution, the frequency of the second peak is compatible with ν_1, while the third and fourth peaks are at the frequencies corresponding to the second and third harmonics of ν_2 (i.e., $2\,\nu_2$ and $3\,\nu_2$, respectively). The natural interpretation of this result based on the Fourier theorem is that $f_{\rm Edd}$ is the composition of two periodic signals, with periodicities ν_1 and ν_2.

As an additional proof for the "physical" nature of the variability of $f_{\rm Edd}$, we computed an "a posteriori" estimate of $f_{\rm Edd}$ by averaging the gas properties in the vicinity of the secondary every 2.5×10^4 yr and then the using these averages to estimate the accretion rates. This approach allowed us to eliminate the effects of the sampling noise due to a finite number of SPH particles. More specifically, we computed the mean values of the density, relative velocity, and temperature of the gas inside the sphere of radius $R_{\rm p} = 7$ pc centered around M_2. The choice of the radius $R_{\rm p}$ is motivated by two arguments: $R_{\rm p}$ is small enough to resolve the substructures in the disc caused by the orbiting MBH, and large enough to have a statistically large number of particles within $R_{\rm p}$ from M_2. The average number of particles inside the sphere defined by $R_{\rm p}$ is $\approx 20,000$, and the minimum number during the whole run is $\approx 2,000$ (i.e., $\approx 60 \times N_{\rm neigh}$). Such large numbers assure that the finite sampling of our disc does not affect our a posteriori estimate. Note that for counter–rotating M_2, $R_{\rm p} > R_{\rm BHL}$. From these properties we estimated the Bondi-Hoyle-Littleton accretion rate onto M_2. The power spectrum of the fluctuations of the new estimated $f_{\rm Edd}$ is shown in Fig. 4 as a blue dot–dashed line. The positions of the second, third and fourth peaks are compatible with the ν_2 and its higher harmonics. The position of the first peak, different from the one found for our original data, can be explained considering that during the first phase of the first orbit M_2 has not yet developed a parsec–scale overdensity in the gas. Consequently, $f_{\rm Edd}$ computed at large separations (i.e., within $R_{\rm p}$) during the first orbit leads to lower signal in the frequency domain at ν_1 compared to the one obtained considering only bound particles (black curve). Note that despite this (expected) difference, the spectrum computed from the unaveraged data does possess a peak at $\nu = \nu_1$, implying a physical origin of variability.

In summary, the two tests discussed in this section prove the "physical" nature of the $f_{\rm Edd}$ variability. The cause of such variability is discussed in the next section.

4 DISCUSSION

For the first time, we are able to study the dynamical evolution of MBHs on retrograde orbits embeded in circumnuclear disks. These simulations require extremely high spatial resolution ($\lesssim 0.1$ pc). We discovered that dynamical friction acting on a MBH moving on an initially retrograde orbit with respect to the disc material leads to an orbital angular momentum flip. The moving MBH always ends up on a prograde orbit by the time the MBH pair forms a binary system (i.e., by the time the gas mass enclosed inside the MBH orbit is smaller than the sum of the MBH masses). We also find that the circularization of the initially eccentric prograde orbit of the secondary is efficient well before the formation of the binary. We stress that the orbital angular momentum flip can only be captured provided that the numerical resolution is sufficiently high.

The dynamical range of our simulations also allowed us

[‡] In run CRE M_2 is counter–rotating for less than 2 orbits, so the Fourier analysis in this case would not be meaningful.

[§] The Nyquist critical frequency in the units of the plot is ≈ 20, well outside the range of ν discussed in this section.

to resolve the sphere of influence of the MBHs and thus, for the first time, study the mass accretion rate of the MBH co- and counter-rotating with respect to the disc. We found that a highly variable double nuclear activity can be observed for few Myr when the two MBHs orbit each other with relative separations $\gtrsim 10$ pc. The accretion history of the moving MBH (M_2) can be divided into two distinct phases. The first stage occurs when the MBH is either on an eccentric co–rotating orbit or on a retrograde orbit irrespective of its eccentricity. The second stage occurs after the circularization of the orbit or after the orbital angular momentum flip of M_2. In the first stage, the accretion rate of the secondary on a counter–rotating orbit is more variable, and its luminosity lower by a factor of a few, than in a co–rotating case. In the second stage, the accretion rate onto the moving MBH is much enchanced. Interestingly, the accretion rate of a MBH that is initially on a counter–rotating orbit exhibits a significantly more rapid transition to the high-mass accretion rate, low-variability state. The luminosity increases by an order of magnitude.

We emphasise that the estimated accretion rate is computed on scales resolved by the simulations. We assume that the accretion rate is stationary. The validity of this assumption depends on the accretion disc physics on unresolved scales, involving physical processes (i.e., magnetohydrodynamics and microscopic transport processes) not implemented in our runs. A fully self–consistent study of the accretion onto the two MBHs down to few gravitational radii is beyond the scope of this investigation.

The reason for the extreme variability in the earlier merger stage (out of the two described above) is twofold. Firstly, the mass accretion fluctuations are driven by the fast fluctuations in the relative velocity between M_2 and the gas environment, that change the $R_{\rm BHL}$ of M_2, and by the inhomogeneities in the gas that passes in the vicinity of the secondary MBH.

Secondly, in the counter–rotating cases, the finite number of gas particles that we use to sample the gas distribution may occasionally lead to short quiescence periods when the secondary is not accreting. In such situations, the $R_{\rm BHL}$ of the secondary is not resolved for a brief time due to the extremly high relative velocity of the MBH with respect to the environment. The finite sampling implies also that values of $f_{\rm Edd}$ of order of 10^{-2} should be considered order of magnitude estimates, and can be incorrect by a factor of a few. However, values of $f_{\rm Edd}$ larger than 0.1 have only a small relative numerical error of $\lesssim 10\,\%$. Therefore, the general dependencies of the luminosity variability on the initial merger parameters are robust. A MBH orbiting in a circumnuclear disc during the final stages of a galaxy merger is expected to be embedded in a gaseous/stellar envelope comoving with the MBH itself. An accurate estimate of the amount of the gas and stars embedding the retrograde MBH depends on the initial conditions of the galaxy merger, and on the interplay between different physical processes, e.g., tidal and ram–pressure stripping. The presence of the stars and gas comoving with the MBH would increase the mass that perturbs the circumnuclear disc and, as a consequence, increase the effect of dynamical friction. This may reduce the timescale of the orbital angular momentum flip. An envelope of gas comoving with M_2 can also increase the accretion rate onto the MBH, and decrease the variability of the accretion process, until the envelope is not totally accreted by M_2 or removed by gravitational/ram–pressure stripping processes. We plan to study such effects in a future paper.

The significant differences between $f_{\rm Edd}$ for MBH on eccentric and circular orbits, and even stronger differences between $f_{\rm Edd}$ in prograde and retrograde cases, can be considered a possible explanation for the paucity of resolved double AGNs in circumnuclear discs. More specifically, it is conceivable that a circumnuclear disk in a galaxy that underwent a merger may host a pair of MBH, but only one of them may show clear signatures of an AGN. Alternatively, the secondary may be significantly dimmer, but highly variable. Such scenarios may occur when the M_2 enters the disc on a counter–rotating trajectory. Such effects have important implications for predicting the rates of double AGN detections in galaxies.

This study opens the way to predicting the properties of the accretion flows near the horizons of the coalescing MBH. Our simulations predict the amount of gas delivered to the very vicinity of the inspiraling MBH. As such our simulations serve as initial conditions required to model the properties of the electromagnetic counterparts to the gravitational wave emission events that will be detectable with the *Laser Interferometer Space Antenna (LISA)* (Armitage & Natarajan 2002; Kocsis et al. 2005; Milosavljevic & Phinney 2005, Dotti et al. 2006a; Lippai, Frei & Haiman 2008; Schnittman & Krolik 2008; Haiman, Kocsis & Menou 2008). We plan to improve upon our model by including gas cooling and heating, star formation and supernova feedback from newly formed stars. These new features can change the structure of the circumnuclear disc, creating a less homogeneous multiphase environment (see, e.g., Wada & Norman 2001, Wada 2004). The interaction between the two MBH and such a multiphase medium can in principle lead to a larger eccentricity of the forming binary, and to more variable accretion events onto the two MBH.

ACKNOWLEDGMENTS

The authors acknowledge the anonymous referee for helpful comments. MD wish to thank Roberto Decarli, David Merritt, Mark Reynolds, Alberto Sesana, and Sandor Van Wassenhove for fruitful suggestions. MR acknowledges *Chandra* Theory grant TM8-9011X. Support for this work was provided by NASA grant NNX07AH22G and SAO-G07-8138 C (MV).

REFERENCES

Armitage P.J., Natarajan P., 2002, ApJ, 567, L9
Armitage P.J., Natarajan P., 2005, ApJ, 634, 921
Ballo L., Braito V., Della Ceca R., Maraschi L., Tavecchio F., Dadina M. 2004, ApJ, 600, 634
Balsara D.W., 1995, J. Comp. Phys., 121, 357
Begelman M.C., Blandford R.D., Rees, M.J., 1980, Nature, 287, 307
Bianchi S., Chiaberge M., Piconcelli E., Guainazzi M., Matt G., 2008, MNRAS, 386, 105
Bogdanovic T., Eracleous M., Sigurdsson S., accepted to ApJ

Comerford J.M., et al., submitted to ApJ (arXiv:0810.3235)
Cuadra J., Armitage P.J., Alexander R.D., Begelman M.C., 2009, MNRAS, 393, 1423
Davies R.I., Tacconi L.J., Genzel R., 2004, ApJ, 613, 781
Decarli R., Gavazzi G., Arosio I., Cortese L., Boselli A., Bonfanti C., Colpi M., MNRAS, 381, 136
Di Matteo T., Springel V., Hernquist L., 2005, Nature, 2005, 433, 604
Dotti M., Colpi M., Haardt F., 2006b, MNRAS, 367, 103
Dotti M., Salvaterra R., Sesana A., Colpi M., Haardt F., 2006a, MNRAS, 372, 869
Dotti M., Colpi M., Haardt F., Mayer L., 2007, MNRAS, 379, 956
Dotti M., Montuori C., Decarli R., Volonteri M., Colpi M., Haardt F., submitted to MNRAS
Downes D., Solomon P.M., 1998, ApJ, 507, 615
Escala A., Larson R.B., Coppi P.S., Maradones D., 2005, ApJ, 630, 152
Ferrarese L., Côté P., Dalla Bontà E., Peng E.W., Merritt D., Jordán A., Blakeslee J.P., Hasegan M., et al., 2006, ApJ Letters, 644, 21
Ferrarese L., 2006, in Series in High Energy Physics, Cosmology and Gravitation, 'Joint Evolution of Black Holes and Galaxies', ed. by M. Colpi, V. Gorini, F. Haardt, U. Moschella (New York - London: Taylor & Francis Group), 1
Foreman G., Volonteri M., Dotti M., 2008, ApJ in press
Haiman Z., Kocsis B., Menou K., submitted to ApJ (arXiv:0807.4697)
Hayasaki K., Mineshige S., Sudou H., 2007, PASJ, 59, 427
Hayasaki K., Mineshige S., Ho L.C., 2008, ApJ, 682, 1134
Hopkins P.F., Hernquist L., Martini P., Cox T. J., Robertson B., Di Matteo T., Springel V., 2005, ApJ, 625, L71
Hopkins P.F., Hernquist L., Cox T.J., Di Matteo T., Robertson B., Springel V., 2006, ApJS, 163, 1
Kazantzidis S. et al., 2005, ApJ, 623, L67
Klessen R.S., Spaans M., Jappsen A., 2007, MNRAS, 374, L29
Kocsis B., Frei Z., Haiman Z., Menou K., 2005, ApJ, 637, 27
Komossa S., Burwitz V., Hasinger G., Predehl P., Kaastra J.S., Ikebe Y., 2003, ApJ, 582, L15
Lippai Z., Frei Z., Haiman Z., 2008, ApJ, 676, L5
Lodato G., Rice W.K.M., 2004, MNRAS, 351, L630
Marconi A., Risaliti G., Gilli R., Hunt L.K., Maiolino R., Salvati M., 2004, MNRAS, 351, 169
Mayer L., Kazantzidis S., Madau P., Colpi M., Quinn T., Wadsley J., 2007, Science, 316, 1874
Milosavljevic M., Phinney E. S., 2005, ApJ, 622, L93
Monaghan J.J., Gingold R.A., 1983, J. Comp. Phys., 52, 374
Nelson A.F., 2006, MNRAS, 373, 1039
Richstone D., et al., 1998, Nature, 395, A14
Rodriguez C., Taylor G.B., Zavala R.T., Peck A.B., Pollack L.K., Romani R.W., 2006, ApJ, 646, 49
Sanders D.B., Mirabel I.F., 1996, ARA&A, 34, 749
Schnittman J.D., Krolik J.H., 2008, ApJ, 684, 870
Shankar F., Salucci P., Granato G.L., De Zotti G., Danese L., 2004, MNRAS, 354, 1020
Spaans M., Silk J., 2000, ApJ, 538, 115
Springel V., Yoshida N., White S.D.M., 2001, NewA, 6, 79
Springel V., Di Matteo T., Hernquist L., 2005, ApJ, 622, L9
Steinmetz M., 1996, MNRAS, 278, 1005
Valtonen, M. J. 2007, ApJ, 659, 1074
Volonteri, M., Haardt, F., Madau, P., 2003, ApJ, 582, 559
Wada K., Norman C.A., 2001, ApJ, 547,172
Wada K., 2004, in Coevolution of Black Holes and Galaxies, ed. L.C. Ho, Cambridge University Press, 186